



Contents lists available at SciVerse ScienceDirect

Spectrochimica Acta Part A: Molecular and Biomolecular Spectroscopy

journal homepage: www.elsevier.com/locate/saa

Salen, reduced salen and N-alkylated salen type compounds: Spectral characterization, theoretical investigation and biological studies

P. Jeslin Kanaga Inba, B. Annaraj, S. Thalamuthu, M.A. Neelakantan *

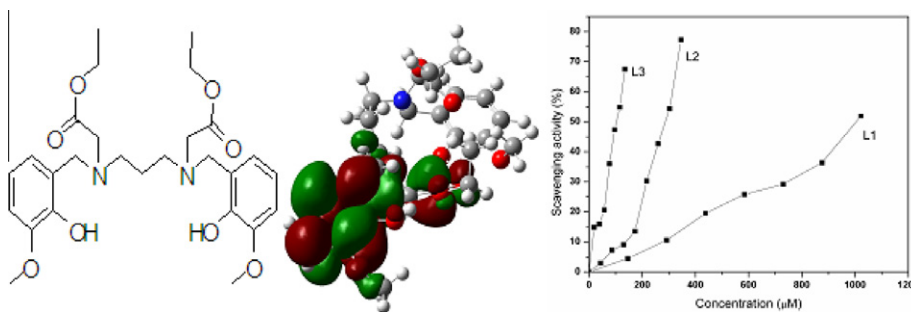
Chemistry Research Centre, National Engineering College, K.R. Nagar, Kovilpatti 628 503, Thoothukudi District, Tamil Nadu, India

HIGHLIGHTS

- ▶ Salen type compounds were synthesized and characterized.
- ▶ Frontier molecular orbitals and vibrational frequencies were computed by DFT/B3LYP.
- ▶ pH and solvent effects on UV–vis spectra of the compounds were studied.
- ▶ DNA binding constants were determined.
- ▶ Antioxidant activities were evaluated.

GRAPHICAL ABSTRACT

Salen type compounds were synthesized and characterized. Molecular geometry of the compounds was optimized by density functional method (B3LYP) with 6-31G basis set. The DNA binding value of the compounds was determined. The antioxidant activity of the compounds was studied using DPPH.



ARTICLE INFO

Article history:

Received 2 November 2012
 Received in revised form 19 November 2012
 Accepted 27 November 2012
 Available online 5 December 2012

Keywords:

Salen type compounds
 Tautomerism
 Solvent effects
 DNA binding properties
 Antioxidant activities

ABSTRACT

Salen [2,2'-(propane-1,3-diylbis[nitrilo(E)methylidene])bis(6-methoxyphenol)], reduced salen [(2,2'-(propane-1,3-diylbis(iminomethylene))bis(6-methoxyphenol))] and N-alkylated salen [diethyl-2,2'-(propane-1,3-diylbis((2-hydroxy-3-methoxybenzyl)azanediyl))diacetate] compounds have been synthesized and characterized by IR, ¹H NMR, ¹³C NMR and UV–vis. spectroscopy. Molecular geometry of the title compounds in the ground state has been optimized by density functional method (B3LYP) with 6-31G basis set. Vibrational frequencies of the compounds were computed and compared with the experimental values. Tautomeric stability study of salen inferred that the enolimine form is more stable than its keto-enamine form in gas phase. The spectral behavior of salen in polar and nonpolar solvents was examined demonstrate the positive solvatochromism. The synthesized compounds have been studied with respect to their binding to calf thymus DNA showed that there were interactions between the compounds and DNA through a groove binding mode. Furthermore, the DNA cleavage activity of the compounds has been investigated by gel electrophoresis. The antioxidant properties of compounds were evaluated by DPPH method. The N-alkylated compound has a higher DPPH free radical scavenging activity. The antimicrobial activity was investigated on various gram positive and gram negative bacteria.

© 2012 Elsevier B.V. All rights reserved.

Introduction

The salen type compounds prepared by the condensation of *o*-hydroxyaldehydes and diamine present versatile, steric, electronic

* Corresponding author. Tel.: +91 9442505839; fax: +91 4632232749.

E-mail addresses: maneels@rediffmail.com, drmaneelakantan@gmail.com (M.A. Neelakantan).

and lipophilic properties [1]. Salen type compounds are used as starting materials in the synthesis of antibiotics, antiallergic, anti-phlogistic and antitumor drugs [2–4]. A prototropic tautomeric attitude has been recognized in 2-hydroxy Schiff bases are of interest mainly due to the existence of OH···N and NH···O type hydrogen bonds. Hydrogen bonding interactions play roles in preferential solvation and have been investigated because it is present in large variety of chemical, biochemical and pharmacolog-

ical events. In salen compounds, the imine nitrogen can act as intramolecular hydrogen bond acceptor and the phenolic oxygen derivatives can act as intermolecular hydrogen bond acceptor. The instability of salen type compounds can be overcome by reduction process. When these compounds are reduced at the imine function, a more flexible, structurally related and basic salen derivatives are obtained [5–7]. N-alkylation of reduced salen gives ester derivatives. Schiff bases containing ester groups show remarkable activity as plant growth hormone [8].

Binding of small molecules to DNA has been studied extensively [9–12]. Small molecules can interact with DNA through non-covalent modes namely, intercalation, groove binding and external electrostatic binding [13–16]. To design effective chemotherapeutic agents and better anticancer drugs, it is essential to explore the interactions of small molecules with DNA. Free radicals play an important role in the oxidative damage of biological systems [17]. They can attack biological molecules such as lipids, proteins, enzymes, DNA and RNA, leading to cell or tissue injury. Therefore estimation of antioxidant activities of the synthesized compounds is important [18].

Despite extensive work has been on salen ligands, little attention has been paid to the reduced salen and N-alkylated salen compounds [19–22]. Hence, in continuation of our earlier works on Schiff bases [23–25], the present investigation reports on the synthesis and spectral characterization of salen, reduced salen and N-alkylated salen compounds. Theoretical investigations of the synthesized compounds were carried out using DFT/B3LYP/6-31G method. This paper also describes the solvatochromism of the synthesized salen in different solvents in the UV–visible spectra. Comparative studies of the interactions of the synthesized compounds with DNA as well as their antioxidant activities were investigated systematically. The experimental results suggest that the synthesized compounds would have potential applications for developing efficient antioxidants.

Experimental

Materials and methods

All chemicals employed for the synthesis were of analytical reagent grade and of highest purity available. *o*-vanillin and 1,3-diaminopropane were purchased from Sigma Aldrich and used as received. Solvents used for the studies were purified and dried by standard procedures. CT DNA and pUC19 DNA were purchased from Genei, Bangalore and used without purification. Tris HCl and ethidium bromide were obtained from HiMedia. Tris HCl–NaCl buffer solution was prepared with double distilled water. 2,2-diphenyl-1-picryl-hydrazyl (DPPH) was purchased from Aldrich.

Microanalytical data were obtained on a Thermo Finnigan Flash EA 1112 series CHN analyzer for C, H and N. The infrared (FT-IR) spectra were recorded on a FTIR Shimadzu 8400S spectrophotometer in the region 4000–400 cm^{-1} . The ^1H and ^{13}C NMR of the compounds in CDCl_3 were recorded on Bruker AV 300 MHz. The electronic spectra were recorded from 200 to 500 nm using Shimadzu UV-2450 spectrophotometer at room temperature.

Synthesis of salen (L1), reduced salen (L2) and N-alkylated salen (L3) compounds

Synthesis of the title compounds is shown in Scheme 1.

Synthesis of 2,2'-[propane-1,3-diylbis[nitrilo(E)methylydene]]bis(6-methoxyphenol) (L1)

o-vanillin (20 mmol, 3.04 g) dissolved in chloroform (25 mL) was mixed with 1,3-diaminopropane (10 mmol, 0.833 mL) in

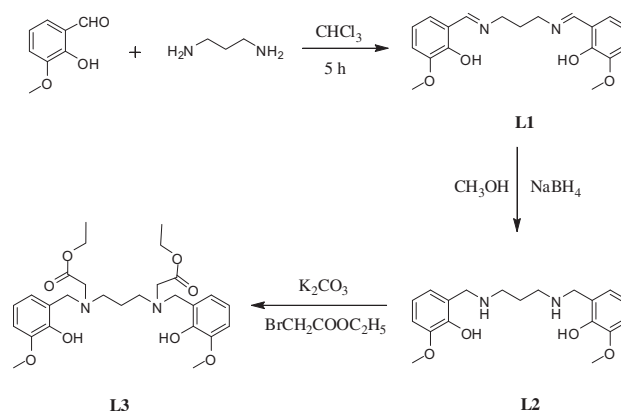
chloroform (25 mL). A brownish yellow colored solution was obtained. The resulting reaction mixture was stirred well at room temperature for 5 h and evaporated under vacuum to remove the solvent. The solution was kept in a refrigerator for 2 days when yellow colored solid precipitate of salen (L1) obtained. Then it was filtered, washed with cold ethanol several times and dried and finally preserved in a desiccator as a yellow solid. Yield: 88%; m.p. 135 °C; Anal. calcd. for $\text{C}_{19}\text{H}_{22}\text{N}_2\text{O}_4$: C, 66.65; H, 6.48; N, 8.18%; Found: C, 66.28; H, 6.29; N, 8.01%. IR (KBr), cm^{-1} : 3448, 3290, 2945, 1631, 1467, 1384, 1271, 1082. ^1H NMR (300 MHz, CDCl_3): δ_{H} = 13.9 (2H, s, OH), 8.3 (2H, s, CH=N), 6.7–6.9 (6H, m, Ar–H), 3.9 (6H, s, $-\text{OCH}_3$), 3.7 (4H, s, N– CH_2), 2.1 (2H, s, CH_2). λ_{max} : 221, 265, 339, 430 nm.

Synthesis of 2,2'-[propane-1,3-diylbis(iminomethylene)]bis(6-methoxyphenol) (L2)

Approximately 2 g (5 mmol) of the salen (L1) was dissolved in 30 mL methanol and sodium borohydride was added drop wise until the formation of a colorless solution. The resulting solution was stirred well at room temperature. After 5 h, the solution was extracted with chloroform and the extracted organic layer was washed with saturated ammonium chloride solution, dried over anhydrous Na_2SO_4 , evaporated under vacuum to remove the solvent and kept on the bench for 24 h. The white colored precipitate formed at the end of this period was the reduced salen (L2). Yield: 80%; m.p. 107 °C; Anal. calcd. for $\text{C}_{19}\text{H}_{26}\text{N}_2\text{O}_4$: C, 65.87; H, 7.56; N, 8.09%; Found: C, 65.52; H, 7.38; N, 7.98%. IR (KBr), cm^{-1} : 3419, 3230, 3323 1271, 1236, 1107, 1084. ^1H NMR (300 MHz, CDCl_3): δ_{H} = 6.6–6.8 (6H, m, Ar–H), 4.1 (4H, s, CH_2 –NH), 3.8 (6H, s, $-\text{OCH}_3$), 2.7 (4H, s, NH– CH_2), 2.2 (2H, s, $-\text{NH}$), 1.8 (2H, s, $-\text{CH}_2$). λ_{max} : 275, 345 nm.

Synthesis of diethyl-2,2'-(propane-1,3-diylbis((2-hydroxy-3-methoxybenzyl) azanediy))diacetate (L3)

Approximately 2 g (5 mmol) of the reduced salen (L2) was dissolved in 20 mL acetonitrile by mixing and potassium carbonate (4.1 g, 30 mmol) was added. The mixture was stirred well under nitrogen atmosphere. Then ethylbromoacetate (3.19 mL, 25 mmol) was added drop wise and stirring was continued for 24 h. The resulting solution was extracted and washed with chloroform and water. The organic layer was separated and dried using anhydrous Na_2SO_4 , filtered and evaporated in vacuum. The filtrate was allowed to stand overnight in air when a semisolid mass appeared at the bottom. The solvent was evaporated off to give the ester (L3) as pale brown oil. The product obtained was purified by column chromatography and is obtained as yellow oil. Yield: 60%; Anal. Calcd. for $\text{C}_{27}\text{H}_{38}\text{N}_2\text{O}_8$: C, 62.53; H, 7.38; N, 5.40%; Found: C,



Scheme 1. Synthesis of the salen type compounds (L1–L3).

Table 1
The experimental and computed vibrational frequencies of salen (L1), reduced salen (L2) and N-alkylated salen (L3) compounds (cm^{-1}).

| Assignments | L1 | | L2 | | L3 | |
|-----------------------------------|--------------|------------|--------------|------------|--------------|-----------|
| | Experimental | DFT/ B3LYP | Experimental | DFT/ B3LYP | Experimental | DFT/B3LYP |
| O–H str | 3448 | 3775 | 3419 | 3589 | 3441 | 3464 |
| C–H (aromatic) stretching | 3290 | 3346 | 3279 | 3236 | 3293 | 3229 |
| C–H (CH_2) stretching | 2945,2839 | 3271,3243 | 2928 | 3104 | 2933 | 3000 |
| C=N stretching | 1631 | 1832 | – | – | – | – |
| C–N stretching | – | – | 1107 | 1299 | 1193 | 1292 |
| N–H stretching | – | – | 3323,3230 | 3478 | – | – |
| C=C (aromatic) stretching | 1467 | 1728 | 1479 | 1520 | 1479 | 1527 |
| C=O (ester) | – | – | – | – | 1747 | 1714 |
| C–O (phenolic) stretching | 1271 | 1582 | 1271 | 1423 | 1280 | 1368 |
| C–O–C sym. stretching | 1082 | 1340 | 1076 | 1175 | 1084 | 1189 |
| C–O–C asym. stretching | 1255 | 1534 | 1236 | 1389 | 1273 | 1347 |
| O–H bend (in plane) | 1384,1359 | 1492,1444 | 1384,1352 | 1492 | 1379 | 1478 |
| O–H bend (out of plane) | 742 | 926 | 729 | 912 | 754 | 863 |
| C–H(aromatic) bend (in plane) | 1170 | 1382 | 1186 | 1230 | 1184 | 1264 |
| C–H(aromatic) bend (out of plane) | 881, 837 | 1077,974 | 833 | 1008 | 860 | 1029 |

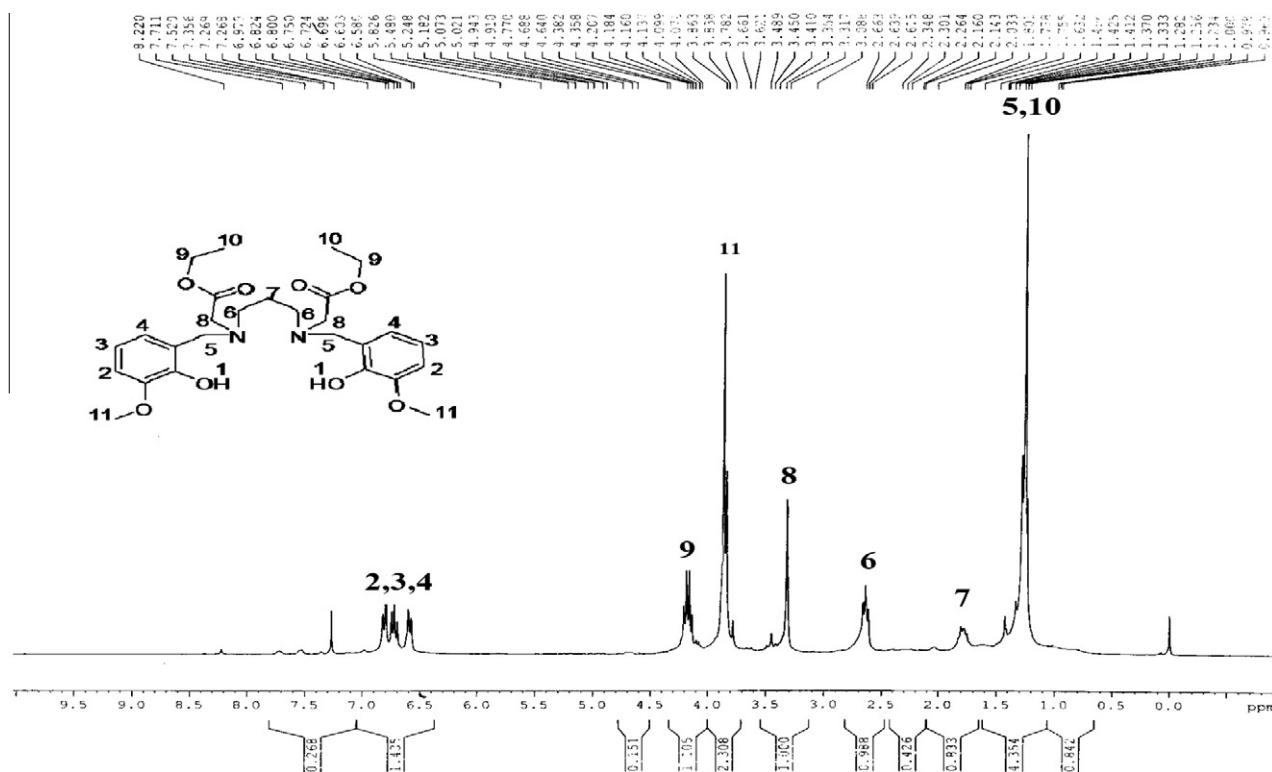


Fig. 1. ^1H NMR spectrum of N-alkylated salen (L3) in CDCl_3 .

62.35; H, 7.25; N, 5.28%. IR (KBr), cm^{-1} : 3441, 3293, 1747, 1280, 1273, 1193, 1084. ^1H NMR (300 MHz, CDCl_3): δ_{H} = 6.5–6.8 (6H, m, Ar–H), 4.2 (4H, s, CH_2CH_3), 3.8 (6H, s, OCH_3), 3.6 (4H, s, $\text{CH}_2\text{–N}$), 3.4 (4H, s, $\text{–NCH}_2\text{COO}$), 2.6 (4H, s, $\text{–NCH}_2\text{CH}_2$), 1.8 (2H, s, $\text{–NCH}_2\text{–CH}_2$), 1.2 (6H, s, –CH_3). ^{13}C NMR (300 MHz, CDCl_3): δ_{C} = 174.12 (COO), 156.51 (C–OH), 151.41 (C– OCH_3), 61.85 (OCH_2CH_3), 59.12 (NCH_2COO), 54.20 (CH_2N), 45.37 (NCH_2CH_2), 23.04 (OCH_2CH_3). λ_{max} : 267, 333 nm.

Computational details

All computations were performed using Gaussian 03W program running under Windows XP. Full geometry optimization of the title compounds was performed by using Density Functional Theory

(DFT) method with Becke's three-parameters hybrid functional using Lee–Yang–Par correlation functional (B3LYP) employing 6-31G basis set as implemented in Gaussian 03W [26]. In addition, vibrational frequencies were computed at the corresponding optimized geometry using the same theory level. The vibrational frequencies calculations showed no imaginary frequencies that ascertained the optimized structure were stable. Total energy and HOMO and LUMO energies for the title compounds (L1–L3) were obtained at B3LYP/6-31G level.

DNA binding measurements

The DNA binding experiments were performed at room temperature. Buffer solution 5 mM Tris HCl and 50 mM NaCl were used for

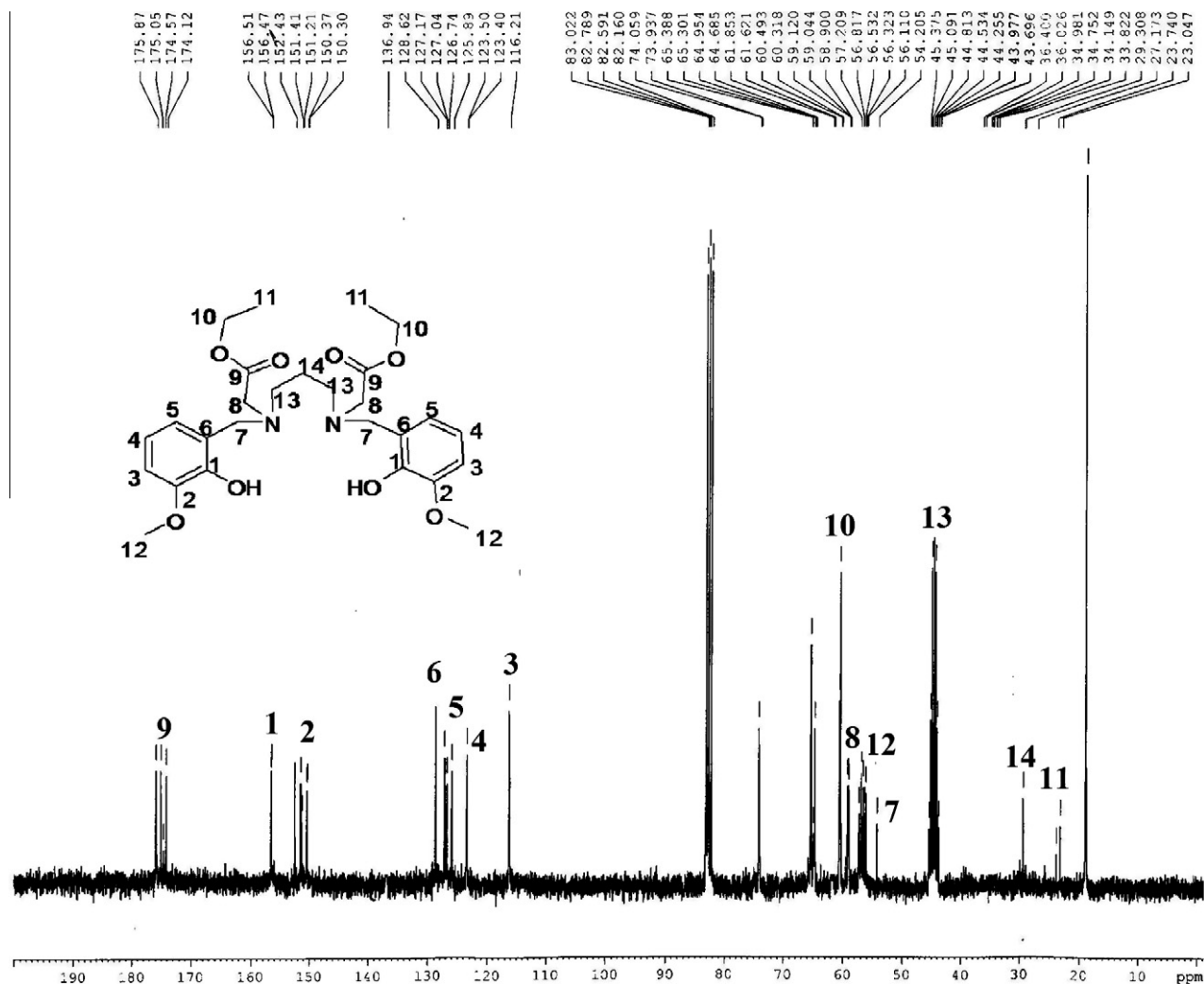
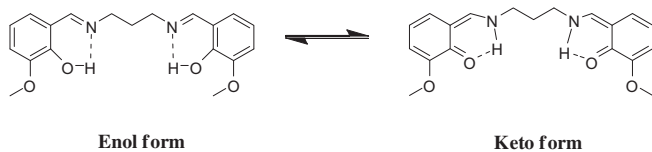


Fig. 2. ^{13}C NMR spectrum of N-alkylated salen (L3) in CDCl_3 .



Scheme 2. Keto-enol tautomerism of salen, L1.

the absorption titrations. A solution of CT DNA in the buffer gave a ratio of UV absorbance at 260 and 280 nm of about 1.8–1.9:1, indicating that the CT DNA was sufficiently free from protein [27]. The concentration of DNA was measured using its extinction coefficient at 260 nm ($6600 \text{ mol L}^{-1} \text{ cm}^{-1}$) [28]. Stock solutions were stored at 4°C and used within 4 days. Concentrated stock solutions of the compounds were prepared by dissolving the compounds in DMSO and diluting suitably with the buffer to the required concentrations for all the experiments. The absorption titrations of the compounds in buffer were performed using a fixed concentration ($20 \mu\text{M}$) to which increments of the DNA stock solution were added ($R = \frac{[\text{DNA}]}{[\text{Compound}]} = 0, 2, 4, 6, 8$ and 10). Compound–DNA solutions were allowed to incubate for 30 min before the absorption spectra were recorded. From the absorption data, the intrinsic binding constant K_b was determined using the equation [29]

$$\frac{[\text{DNA}]}{(\varepsilon_a - \varepsilon_f)} = \frac{[\text{DNA}]}{(\varepsilon_b - \varepsilon_f)} + \frac{1}{K_b(\varepsilon_b - \varepsilon_f)} \quad (1)$$

where ε_a , ε_f and ε_b are the apparent, free and bound compound extinction coefficients respectively. In the plots of $\frac{[\text{DNA}]}{(\varepsilon_a - \varepsilon_f)}$ versus $[\text{DNA}]$, K_b is given by the ratio of slope to the intercept.

DNA cleavage experiment

The DNA cleavage experiment was conducted using pUC 19 DNA by gel electrophoresis with the corresponding compound in the presence of H_2O_2 as oxidant. The reaction mixture was prepared as follows: $10 \mu\text{L}$ of pUC 19 DNA, $5 \mu\text{L}$ of the compound in DMSO, $1 \mu\text{L}$ of H_2O_2 followed by dilution with buffer 50 mM Tris–HCl and 50 mM NaCl to a total volume of $25 \mu\text{L}$. The samples were incubated at 37°C for 1 h in the presence and absence of the compound. It is then loaded on 1% agarose gel after mixing with $3 \mu\text{L}$ of loading dye (0.25% bromophenol and 40% sucrose). The samples were electrophoresed at 100 V using Tris-boric acid-EDTA buffer ($\text{pH} = 8.0$) until the bromophenol blue reached to one third of the gel. The gel was stained using ethidium bromide for 10 min and the bands were visualized and photographed under a UV Trans illuminator.

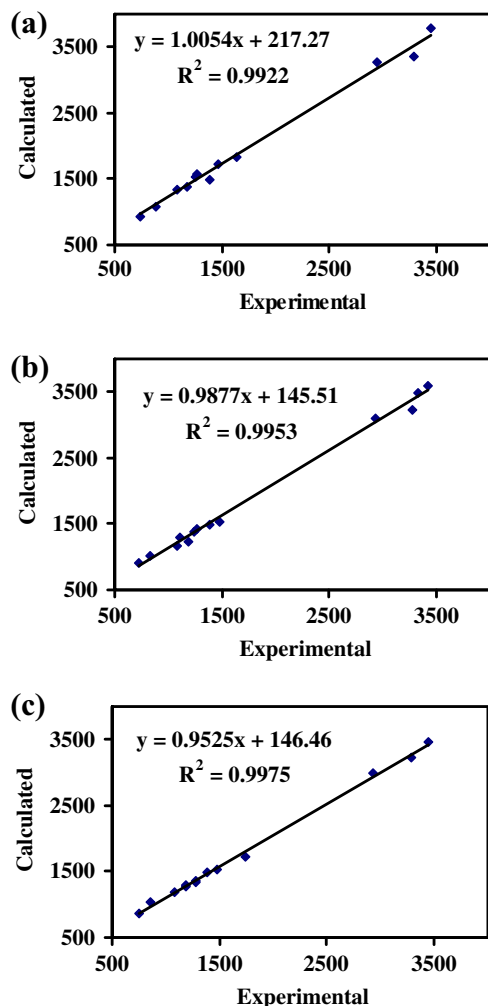


Fig. 3. Correlation graphs of calculated and experimental IR frequencies of: (a) L1 (b) L2 and (c) L3.

Antioxidant property

Antioxidant activity of the synthesized compounds was expressed from their radical scavenging ability against the stable free radical, 2,2-diphenyl-1-picrylhydrazyl (DPPH \cdot). The DPPH \cdot scavenging capacity was measured according to the following procedure [30,31]. The concentration of DPPH \cdot used for antioxidant activity was 50 μ M. Different concentrations of the synthesized compounds in methanol was added to DPPH \cdot in methanol solution. The reaction tubes were wrapped in aluminum foil and shaken vigorously and kept at room temperature for 30 min in dark. The reduction of the DPPH \cdot was monitored by observing the decrease in absorbance at 517 nm using a spectrophotometer. The radical scavenging capacity of the antioxidants was expressed in terms of % inhibition and IC₅₀. The capability to scavenge the DPPH \cdot was calculated using the following equation [32].

$$\% \text{ Inhibition} = \frac{(A_{\text{control}} - A_{\text{sample}})}{A_{\text{control}}} \times 100 \quad (2)$$

where A_{control} is the absorbance of DPPH \cdot in methanol solution without an antioxidant, and A_{sample} is the absorbance of DPPH \cdot in the presence of an antioxidant. The IC₅₀ value is the concentration of the antioxidant required to scavenge 50% DPPH \cdot and is calculated from the inhibition curve.

Antimicrobial activity

The ligands **L1**, **L2** and **L3** were tested for their *in vitro* antibacterial activity against *Streptococcus pyogenes* and *Staphylococcus* as Gram positive bacteria and *Escherichia Coli*, *Klebsiella*, *Aeromonas* and *Serratia* as Gram negative bacteria by well diffusion method [33] using Ampicillin and Amoxicillin as standards. The liquid medium containing the bacterial subcultures was autoclaved for 20 min at 121 °C and at 15 lb pressure before inoculation. The bacteria were then cultured for 24 h at 37 °C in an incubator. Mueller–Hinton nutrient agar was poured over sterile 90 mm Petri dishes and allowed to solidify. Wells were made on the agar medium inoculated with microorganism. The test compounds in DMSO solution were added into the well using suitable techniques and the plates were incubated at 24 h at 37 °C. During this period, the test solution diffused and the growth of the inoculated microorganism was affected. The inhibition zone was developed and measured at the end of the incubation period. Experiments were performed in triplicate and standard deviation was calculated.

Results and discussion

All the synthesized compounds are stable at room temperature. The compounds are soluble in most of the organic solvents and insoluble in water. The analytical data of the compounds are given in Section 2.

IR spectra

The FT-IR spectral data of the title compounds (L1–L3) are given in Table 1 and Fig. S1. The IR spectrum of the salen, L1 exhibits a broad band centered at 3448 cm^{-1} is due to the formation of strong intramolecular and intermolecular hydrogen bonding of phenolic –OH group. A strong band at 1631 cm^{-1} is due to the azomethine group vibration. The C–O stretching vibration of the phenolic part of *o*-vanillin is appeared at 1271 cm^{-1} . In the reduced salen (L2), the spectrum exhibits a medium peak at 3230 cm^{-1} is ascribed to the N–H stretching vibration, confirming that the imine group of the salen has been reduced. The absence of –CH=N– group in L2 is further confirmed from the disappearance of the typical strong band at 1631 cm^{-1} due to imine vibration appears in L1. The band appeared at 1107 cm^{-1} is due to the C–NH vibration of the reduced part of the azomethine group. In the N-alkylated salen (L3), the bands at 1193 and 1747 cm^{-1} can be attributed to the vibrations of the C–N and C=O of ester groups respectively. These data confirms the formation of salen, reduced salen and N-alkylated salen compounds.

^1H and ^{13}C NMR

The ^1H and ^{13}C NMR spectra of L1–L3 were recorded in CDCl_3 . The signal at 8.3 δ observed in L1 can be attributed to the azomethine proton demonstrated the formation of salen compound (L1). The phenolic –OH proton of L1 shows signal at 13.9 δ (Fig. S2). The aromatic protons exhibit multiplets in the 6.7–6.9 range. The methoxy protons show singlet at 3.9 δ . The signals at 3.7 and 2.1 can be attributed to the –CH₂ protons of 1,3-diaminopropane. From these data, the formation of salen (L1) is confirmed. The disappearance of azomethine proton signal at 8.3 and appearance of a new signal at 4.1 (methylene proton of benzyl part) in the spectrum of L2 clearly demonstrates the reduction of azomethine group (L2) (Fig. S3). Aromatic protons give signals in the region 6.6–6.8. The peak at 3.8 is considered as methoxy protons. The signal at 2.7 δ is assigned to α methylene proton of amine part. The peak at 1.8 δ is considered as β methylene protons of the amine part.

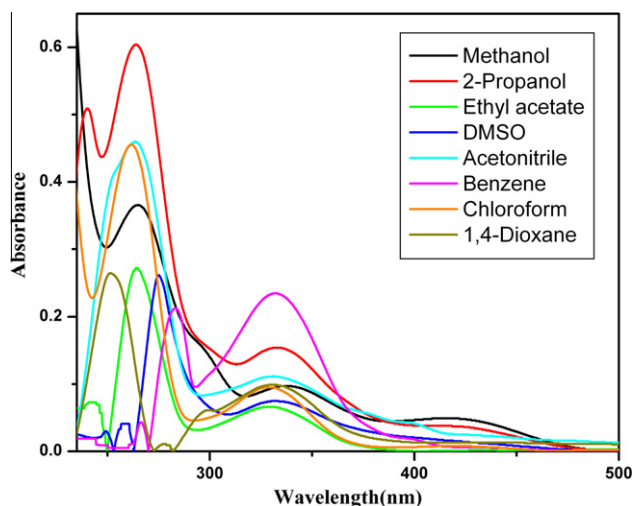


Fig. 5. UV-vis spectra of salen L1 (1×10^{-5} M) in solvents with different polarity range.

Table 3
Electronic spectral data of salen (L1) in polar and nonpolar solvents.

| Solvent | Dielectric constant | Benzene ring $\pi \rightarrow \pi^*$ | Azomethine ring $\pi \rightarrow \pi^*$ | E_{\max} (kcal mol $^{-1}$) |
|--------------------|---------------------|--------------------------------------|---|--------------------------------|
| 1,4-Dioxane | 2.21 | 254 | 329 | 86.90 |
| Benzene | 2.28 | 279 | 332 | 86.12 |
| Chloroform | 4.81 | 261 | 330 | 86.64 |
| Ethyl acetate | 6.0 | 264 | 332 | 86.12 |
| 2-Propanol | 18.3 | 263 | 331 | 86.37 |
| Methanol | 32.6 | 264 | 338 | 84.59 |
| Acetonitrile | 37.5 | 261 | 328 | 87.17 |
| Dimethylsulphoxide | 47 | 272 | 335 | 85.35 |

at 275 nm and 345 nm. The high intensity band at 275 nm is attributed to $\pi \rightarrow \pi^*$ transition of aromatic ring and low intensity band at 345 nm is characteristic of $\pi \rightarrow \pi^*$ transition due to H-bonding induced changes of OH proton-donor aromatic molecules and amine NH [35]. These bands are shifted in N-alkylated salen (L3) and are observed at 267 and 333 nm.

Computational studies

Optimized geometry

The structures of the title compounds have been optimized using the B3LYP method at 6-31G level. The salen compound exists in keto-enol tautomerism. The enolimine (O—H...N) and ketoamine (N—H...O) tautomers for the compound L1 is shown in Scheme 2. To investigate the tautomeric stability, optimization at B3LYP/6-31G level for both enolimine and ketoamine forms of L1 was performed in gas phase. The value of the total energy calculated in gas phase for the enolimine form of L1 is -1147.29060 a.u., which is lower than the ketoamine form (-1147.5713 a.u.). This clearly demonstrates that the enol imine form is more stable than the ketoamine form in gas phase.

Vibrational assignments

Harmonic vibrational frequencies of the title compounds were calculated using the DFT/B3LYP method with the 6-31G basis set using the Gaussian 03W program package [26]. The vibrational band assignments were made using the Gauss-View molecular visualization program. The experimentally observed peaks were

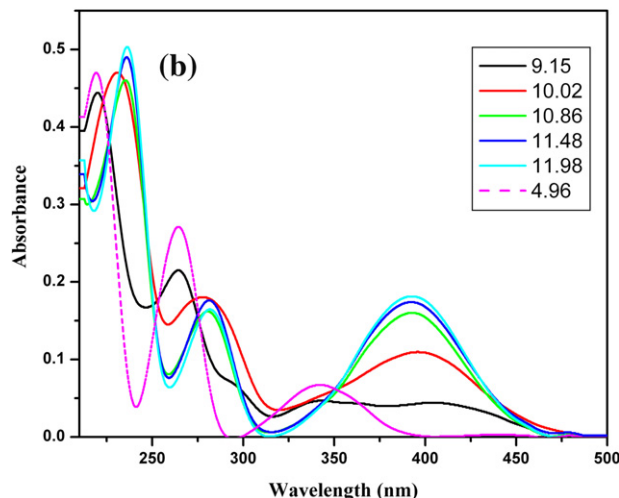
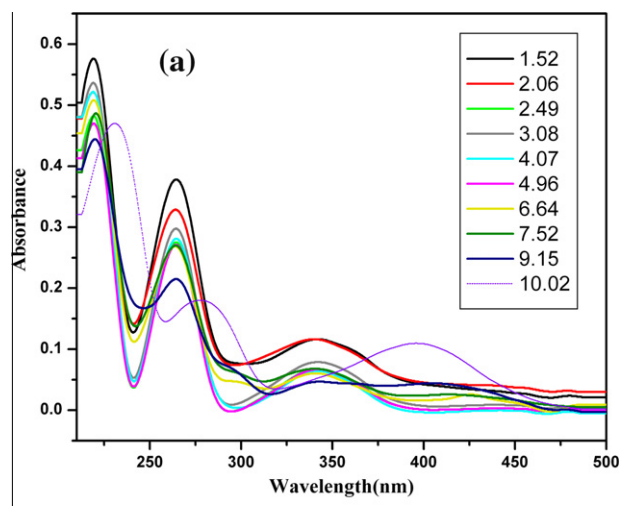


Fig. 6. pH dependent UV-vis. spectra of L1 (a) pH = 1.52–10.02 and (b) pH = 4.96–11.98.

Table 4
Electronic absorption spectral properties of L1–L3 with CT-DNA.

| Compound | λ_{\max} (nm) | | $\Delta\lambda$ (nm) | a H% | K_b (M $^{-1}$) |
|----------|-----------------------|-------|----------------------|---------|--------------------|
| | Free | Bound | | | |
| L1 | 265.4 | 266.8 | 1.4 | 12.07 | 4×10^4 |
| L2 | 279.8 | 281.8 | 2 | 22.20 | 1.25×10^4 |
| L3 | 272.8 | 277.2 | 4.4 | 13.04 | 1.23×10^5 |

$$^a \text{H\%} = [(A_{\text{free}} - A_{\text{bound}}) / A_{\text{free}}] \times 100\%.$$

compared with the calculated results (Table 1). The assignment of the experimental frequencies is based on the observed band frequencies in the infrared spectra by establishing one to one correlation between observed and theoretically calculated frequencies. The calculated frequencies are higher than the observed values for the majority of the normal modes. The reason for the discrepancy between the experimental and computed spectra is that the experimental value is an inharmonic frequency while the calculated value is a harmonic frequency. To make a comparison with the experimental observation, correlation graphs (Fig. 3) were drawn. From the correlation graphs, it is clear that the experimental fundamentals are found to have good correlation with the computed values.

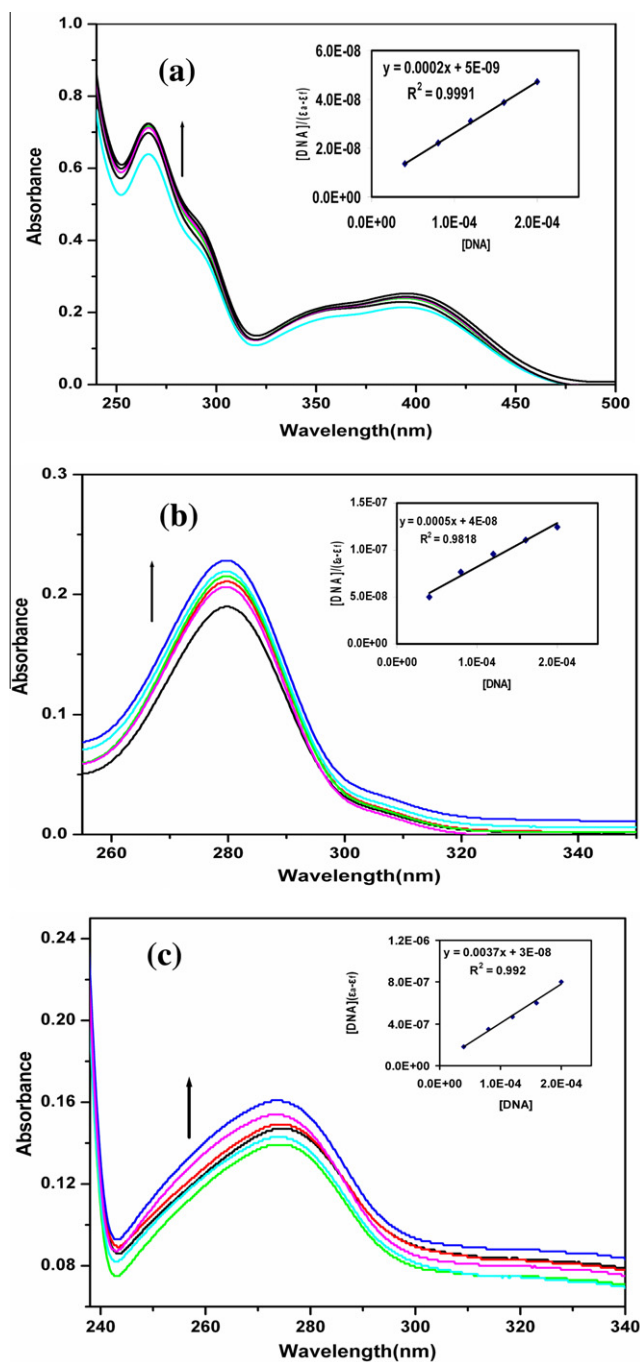


Fig. 7. Absorption spectra of: (a) L1 (b) L2 and (c) L3 (20 μM) in 5 mM Tris-HCl buffer at pH = 7.2, in the absence ($R=0$) and presence ($R=2, 4, 6, 8$ and 10) of increasing amounts of CT DNA. Arrow shows the intensity changes upon increasing DNA concentration. Inset: Plot of $[\text{DNA}]/\epsilon_0-\epsilon_x$ versus $[\text{DNA}]$.

Frontier molecular orbitals

The electronic absorption corresponds to the transition from ground to the first excited state and is mainly described by one electron excitation from the highest occupied molecular orbital (HOMO) to the lowest unoccupied molecular orbital (LUMO) [36]. Fig. 4 shows the distributions and energy levels of the HOMO - 1, HOMO, LUMO, and LUMO - 1 orbitals computed at the B3LYP/6-31G level for the title compounds. From the HOMO-LUMO orbital picture, the filled π orbital (HOMO) is mostly located in between the aromatic ring and the unfilled π^* orbital (LUMO) on the aromatic ring. Consequently, the HOMO \rightarrow LUMO transition

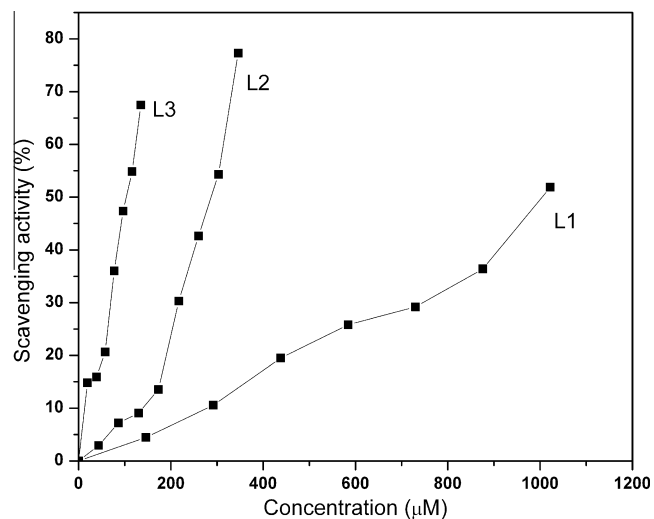


Fig. 8. Trends in the inhibition of DPPH radicals by L1, L2 and L3 at different concentrations.

Table 5

The antibacterial activities of L1–L3 by well diffusion method (zone formation in mm, standard deviation ± 2).

| Bacterial strains | Diameter of inhibition zone of bacteria in different compounds | | | | |
|-----------------------|--|----|----|------------|-------------|
| | L1 | L2 | L3 | Ampicillin | Amoxicillin |
| <i>S. pyogenes</i> | 13 | 5 | 5 | 16 | 14 |
| <i>Staphylococcus</i> | 14 | 6 | 8 | 10 | 10 |
| <i>E. Coli</i> | 11 | 10 | R | 12 | 14 |
| <i>Klebsiella</i> | 12 | R | R | 14 | 16 |
| <i>Aeromonas</i> | 8 | 5 | 7 | 12 | 10 |
| <i>Serratia</i> | 14 | 6 | 8 | 10 | 10 |

R – Resistant.

implies an electron density transfer to the C–C bond of the benzene ring from $\text{CH}_2\text{-NH}$ group. The HOMO–LUMO energy gap was calculated at DFT-B3LYP method using 6-31G basis set (Table 2) reflects the chemical activity of the molecule. The LUMO as an electron acceptor represents the ability to obtain an electron and HOMO represents the ability to donate an electron. The smaller the LUMO and HOMO energy gap computed in the present investigation suggests that the HOMO electrons can be easily excited. Moreover, a lower HOMO–LUMO energy gap explains the fact that eventual charge transfer interaction is taking place within the molecule. The calculated physicochemical properties such as total energies, HOMO and LUMO energies are given in Table 2.

Solvatochromaticity of the salen (L1) in different organic solvents

The salen (L1) shows band at 430 nm in methanol gives information about ketoenol tautomerism of the compound (Fig. 5). The UV–vis spectrum of L1 is taken in polar and non-polar solvents in the 200–500 nm range and the spectral data are summarized in Table 3. The absorption band at 335 nm (in DMSO) and 329 nm (in 1,4-Dioxane) are attributed to $\pi \rightarrow \pi^*$ transitions. However, a new absorption band at 430 nm was observed in the spectrum of L1 in polar protic solvents like methanol and 2-propanol which was not present in the case of nonpolar and polar aprotic solvents. In non-polar solvents, L1 is present predominantly in the enolimine form as confirmed by NMR spectra taken in CDCl_3 . The signals of the hydroxyl and azomethine protons for L1 appear at 13.9 ppm and

8.3 ppm respectively (Fig. S2). Their shapes and positions are characteristic of the enolimine form with a strong intramolecular OH...N=C bond [37]. Thus, the absorption band at 328–338 nm arises from the enolimine form and the band at 430 nm arises from the ketoamine form in solution. The E_{max} values of $\pi \rightarrow \pi^*$ transition of the salen in different solvents were calculated by the following equation [38]:

$$E_{max}(\text{kcal mol}^{-1}) = 28591/\lambda_{max}(\text{nm}) \quad (3)$$

To find the sign, the value of ΔE was calculated from the E_{max} of the most nonpolar solvent and the most polar solvent.

$$\Delta E = E_{max} \text{ of the most nonpolar solvent} \\ - E_{max} \text{ of the most polar solvent}$$

The salen shows a red shift and positive solvatochromism when the polarity of the solvent is increased. This confirms that the molecule is more polarized in the excited state (i.e.) the molecule is stabilized by the polar solvents in the excited state.

UV-vis. spectra of salen (L1) in acidic and basic solutions

The spectrophotometric titration of salen in methanol was carried out in acidic and basic medium to explain the deprotonation process. The spectrum of salen (L1) gives three absorptions in the range 200–500 nm as a function of pH (1.52–11.98). From pH = 1.52 to 7.52, the three peak positions (220, 264 and 341 nm) remain invariant suggests that L1 is in protonated form in this pH range (Fig. 6a). By increasing the pH to 9.15, the absorption at 220 nm is shifted to 239 nm (bathochromic shift), and the other two peaks at 264 and 341 nm start to decrease sharply in intensity and a new peak occurs at 282 and 394 nm. These peaks at 282 and 394 nm grows in intensity up to pH = 11.98 with complete disappearance of the original peaks at 264 and 341 nm (Fig. 6b). These results indicate that L1 is in deprotonated form with pH > 9.15. There are two isosbestic points for the series of curves from pH = 1.52 to 11.98 at 245 nm and 280 nm. At lower pH, L1 is in the protonated form whereas at higher pH L1 is in the deprotonated form.

Biological activities

DNA binding studies

The UV-vis. absorption spectra of the compounds (L1–L3) in buffer solution show intense absorption bands at 265, 280, and 273 nm, respectively (Table 4). These absorption bands are perturbed by the addition of increasing amounts of DNA (Fig. 7). Addition of CT DNA to the test compounds induce hyperchromic responses of about 12.07% at 265 nm for L1, 22.2% at 280 nm for L2 and 13.04% at 273 nm for L3 at $R = 10$. The hyperchromism accompanied by a small shift in λ_{max} is consistent with groove binding leading to small perturbations [39]. In order to compare quantitatively, the binding constants (K_b) were calculated using Eq. (1). The value of K_b determined from the ratio of slope to intercept from the plot of $\frac{[DNA]}{(e_0 - e_f)}$ versus [DNA] is 4×10^4 , 1.25×10^4 and $1.23 \times 10^5 \text{ M}^{-1}$ for L1, L2 and L3 respectively. The magnitude of the binding constant values clearly showed that all the compounds bound with CT DNA and the binding strength increases in the order $L2 < L1 < L3$ (Table 4). These results suggest that molecular features containing N-alkyl group on the side chain are associated with higher affinity binding to DNA. However, the K_b values obtained here are lower than the value reported for the classical intercalator, ethidium bromide [40].

Nuclease activity

The ability of the synthesized compounds to perform DNA cleavage is carried out using pUC19 DNA by agarose gel electrophoresis (Fig. S5). The tests were performed under aerobic conditions at the compound concentration of 40 μM . The cleavage of pUC19 DNA induced by L1, L2 and L3 results in the conversion of supercoiled form (SC) to nicked circular (NC) form. The nuclease activity is measured from the amount of form I (SC) diminish and partly converted to form II (NC) and follows the order $L3 > L1 > L2$. The variation of DNA cleavage efficiency of the synthesized compounds may be due to the different binding affinity of the compound to DNA. The compound with a greater DNA binding propensity shows better nuclease activity.

Antioxidant activity

The antioxidant activity of synthesized compounds was measured in terms of their hydrogen donating or radical scavenging capability against stable radical DPPH \cdot by UV-vis. spectrophotometer. The antioxidants containing phenols (ArOH) react with DPPH \cdot via two different mechanisms: (i) a direct donation of phenol H-atom and (ii) an electron transfer process from ArOH or its phenoxide anion (ArO $^-$) to DPPH \cdot [41]. The pathway of reaction depends upon the nature of the solvent or the redox potentials of the species involved. The experiment was carried out in methanol capable of forming strong hydrogen bonds with the ArOH molecules and the electron transfer mechanism becomes important. The decrease of DPPH \cdot absorbance with addition of compounds results in the scavenging of the radical by electron transfer process from ArOH or its phenoxide anion (ArO $^-$) to DPPH \cdot [42]



All the synthesized compounds show DPPH \cdot radical scavenging capability due to the presence of *o*-methoxy substitution which stabilizes the aryloxy radical [43]. The radical scavenging capacity of the compounds calculated by Eq. (2) and is expressed in terms of IC $_{50}$ (50% inhibitory concentration). The IC $_{50}$ values of L1, L2 and L3 are 1022, 259.8 and 96.4 μM respectively (Fig. 8). Lower value indicates the higher radical scavenging capacity. This implies that the free radical scavenging activity of N-alkylated salen compound is greater than the salen and reduced salen compounds ($L1 < L2 < L3$). The lower IC $_{50}$ value observed for N-alkylated salen demonstrates that the compound has a potential to be applied as scavenger to eliminate the free radicals. However, the IC $_{50}$ values of synthesized compounds are much higher than the positive control like ascorbic acid, 11.55 μM [44].

Antimicrobial activity

The invitro antibacterial activity of the title compounds was tested against six human pathogenic microorganisms, viz., *S. pyogenes* and *Staphylococcus* as gram positive bacteria and *E. Coli*, *Klebsiella*, *Aeromonas* and *Serratia* as gram negative bacteria by well diffusion method using ampicillin and amoxicillin as standards (Table 5). The results of antimicrobial studies of L1, L2 and L3 are given in Fig. S6. A close examination of the results showed that the salen compound, L1 is effective against all the bacteria tested. Also, L1 shows higher activity for *Staphylococcus* and *Serratia* than the control. The reduced salen, L2 does not show any activity against *Klebsiella*, but has moderate activity against other microorganisms. The N-alkylated salen, L3 does not show any activity against *E. Coli* and *Klebsiella* and has moderate activity against other organisms. The remarkable activity of the salen may be due to the presence of the azomethine and hydroxyl groups in the molecule.

Conclusion

In this work, a salen, reduced salen and N-alkylated salen have been synthesized and characterized. The salen in solvent media is found to exist in keto and enol forms. DFT study of salen inferred that the enolimine form is more stable than its ketoamine form in gas phase. The DNA binding results suggest that the synthesized compounds bind to DNA in a groove binding mode. The N-alkylated salen has higher binding ability with DNA than the salen and reduced salen ligand. The compounds have been found to promote cleavage of pUC 19 DNA from the super coiled form to nicked form in presence of H₂O₂. The antioxidant activity evaluated by DPPH radical scavenging method found that N-alkylated salen is much more effective free radical scavenger than the reduced salen and salen. The synthesized compounds possess potential antimicrobial activity.

Acknowledgements

The authors thank Dr.V. Subramanian, Principal Scientist, Chemical Lab., Central Leather Research Institute, Chennai for access to the Gaussian 03 program package. Dr. MAN sincerely thanks the Department of Science and Technology (DST), New Delhi, for providing the UV–visible spectral facility through funding (SR/S1/IC-08/2010).

Appendix A. Supplementary material

Supplementary data associated with this article can be found, in the online version, at <http://dx.doi.org/10.1016/j.saa.2012.11.100>.

References

- [1] I. Correia, J.C. Pessoa, M. Teresa Duarte, M.F. Minas da Piedade, T. Jackush, T. Kiss, M.M.C.A. Castro, C.F.G.C. Geraldés, F. Avecilla, *Eur. J. Inorg. Chem.* (2005) 732–744.
- [2] D. Barton, W.D. Ollis, *Comprehensive Organic Chemistry*, vol. 2, Pergamon Oxford, 1979.
- [3] R.W. Layer, *Chem. Rev.* 63 (1963) 489–510.
- [4] H. Tanaka, A. Agar, M. Yavuz, *J. Mol. Model.* 16 (2010) 577–587.
- [5] M.R.A. Pillai, C.S. John, J.M. Lo, D.E. Troutner, M. Corlija, W.A. Volkert, R.A. Holmes, *Nucl. Med. Biol.* 20 (1993) 211–216.
- [6] Y.S. Xie, Y. Xue, F.P. Kou, R.S. Lin, Q.L. Liu, *J. Coord. Chem.* 53 (2001) 91–97.
- [7] A. Biswas, L. Kanta Das, M.G.B. Drew, G. Aromi, P. Gamez, A. Ghosh, *Inorg. Chem.* 51 (2012) 7993–8001.
- [8] S. Huneck, K. Schreiber, H.T. Grimmecke, *J. Plant Growth Regul.* 3 (1984) 75–84.
- [9] J.K. Barton, *Science* 233 (1986) 727–734.
- [10] P.B. Dervan, *Science* 232 (1986) 464–471.
- [11] W.S. Wade, P.B. Dervan, *J. Am. Chem. Soc.* 109 (1987) 1574–1575.
- [12] K.R. Fox, G.W. Grigg, M.J. Waring, *Biochem. J.* 243 (1987) 847–851.
- [13] R. Vijayalakshmi, M. Kanthimathi, R. Parthasarathi, B.U. Nair, *Bioorg. Med. Chem.* 14 (2006) 3300–3306.
- [14] V.G. Vaidyanathan, B.U. Nair, *J. Inorg. Biochem.* 95 (2003) 334–342.
- [15] A.K. Patra, S. Roy, A.R. Chakravarty, *Inorg. Chim. Acta* 362 (2009) 1591–1599.
- [16] X.B. Yang, Y. Huang, J.S. Zhang, S.K. Yuan, R.Q. Zeng, *Inorg. Chem. Comm.* 13 (2010) 1421–1424.
- [17] M. Valko, C.J. Rhodes, J. Moncol, M. Izakovic, M. Mazur, *Chem. Biol. Interact.* 160 (2006) 1–40.
- [18] M. Valko, D. Leibfritz, J. Moncol, M.T. Cronin, M. Mazur, J. Telser, *Int. J. Biochem. Cell Biol.* 39 (2007) 44–84.
- [19] Namrata T. Shalini, V.K. Sharma, *Polish J. Chem.* 82 (2008) 523–535.
- [20] S. Thakurta, R.J. Butcher, G. Pilet, S. Mitra, *J. Mol. Struct.* 929 (2009) 112–119.
- [21] S. Thakurta, C. Rizzoli, R.J. Butcher, C.J. Gomez-Gracia, E. Garribba, S. Mitra, *Inorg. Chim. Acta* 363 (2010) 1395–1403.
- [22] A.N. Borisov, A.V. Shchukarev, G.A. Shagigultanova, *Russ. J. Appl. Chem.* 82 (2009) 1242–1250.
- [23] B.M. Draskovic, G.A. Bogdanovic, M.A. Neelakantan, A. Chamayou, S. Thalamuthu, Y.S. Avadhut, J.S. Gunne, S. Banerjee, C. Janiak, *Cryst. Growth Des.* 10 (2010) 1665–1676.
- [24] M.A. Neelakantan, S.S. Mariappan, J. Dharmaraja, T. Jeyakumar, K. Muthukumar, *Spectrochim. Acta A* 71 (2008) 628–635.
- [25] V. Selvarani, B. Annaraj, M.A. Neelakantan, S. Sundaramoorthy, D. Velmurugan, *Spectrochim. Acta A* 91 (2012) 329–337.
- [26] M.J. Frisch, G.W. Trucks, H.B. Schlegel, G.E. Scuseria, M.A. Robb, J.R. Cheeseman, J.A. Montgomery, T.J. Vreven, K.N. Kudin, J.C. Burant, J.M. Millam, S.S. Iyengar, J. Tomasi, V. Barone, B. Mennucci, M. Cossi, G. Scalmani, N. Rega, G.A. Petersson, H. Nakatsuji, M. Hada, M. Ehara, K. Toyota, R. Fukuda, J. Hasegawa, M. Ishida, T. Nakajima, Y. Honda, O. Kitao, H. Nakai, M. Klene, X. Li, J.E. Knox, H.P. Hratchian, J.B. Cross, C. Adamo, J. Jaramillo, R. Gomperts, R.E. Stratmann, O. Yazyev, A.J. Austin, R. Cammi, C. Pomelli, J.W. Ochterski, P.Y. Ayala, K. Morokuma, G.A. Voth, P. Salvador, J.J. Dannenberg, V.G. Zakrzewski, S. Dapprich, A.D. Daniels, M.C. Strain, O. Farkas, D.K. Malick, A.D. Rabuck, K. Raghavachari, J.B. Foresman, J.V. Ortiz, Q. Cui, A.G. Baboul, S. Clifford, J. Cioslowski, B.B. Stefanov, G. Liu, A. Liashenko, P. Piskorz, I. Komaromi, R.L. Martin, D.J. Fox, T. Keith, M.A. Al-Laham, C.Y. Peng, A. Nanayakkara, M. Challacombe, P.M.W. Gill, B. Johnson, W. Chen, M.W. Wong, C. Gonzalez, J.A. Pople, Gaussian 03, Revision E. 01, Gaussian, Inc., Wallingford, CT, 2004.
- [27] C. Merrill, D. Goldman, S.A. Sedman, M.H. Ebert, *Science* 211 (1980) 1437–1438.
- [28] M.E. Reichman, S.A. Rice, C.A. Thomas, P. Doty, *J. Am. Chem. Soc.* 76 (1954) 3047–3053.
- [29] A. Wolfe, G.H. Shimer, T. Meehan, *Biochemistry* 26 (1987) 6392–6396.
- [30] M.S. Blois, *Nature* 181 (1958) 1199–1200.
- [31] W.B. Williams, M.E. Cuvelier, C. Berset, *Lebensm. Wiss. Technol.* 28 (1995) 25–30.
- [32] B.M. Lue, N.S. Nielson, *Food Chem.* 123 (2010) 221–230.
- [33] M.J. Pelczar, E.C.S. Chanm, N.R. Krieg, *Microbiology*, Blackwell Science, New York, 1998.
- [34] I.S. Ahmed, M.A. Kassem, *Spectrochim. Acta A* 77 (2010) 359–366.
- [35] H. Baba, S. Suzuki, *J. Chem. Phys.* 35 (1961) 1118–1127.
- [36] S. Jeyavijayan, M. Arivazhagan, *Ind. J. Pure Appl. Phys.* 50 (2012) 623–632.
- [37] N. Galic, Z. Cimerman, V. Tomisi, *Spectrochim. Acta A* 71 (2008) 1274–1280.
- [38] G. Suganthi, S. Sivakolunthu, V. Ramskrishnan, *J. Fluoresc.* 20 (2010) 1181–1189.
- [39] Q.S. Li, P. Yang, H.F. Wang, M.L. Guo, *J. Inorg. Biochem.* 64 (1996) 181–195.
- [40] M.J. Waring, *J. Mol. Biol.* 13 (1965) 269–282.
- [41] M.C. Foti, C. Daquino, C. Geraci, *J. Org. Chem.* 69 (2004) 2309–2314.
- [42] G. Litwinienko, K.U. Ingold, *J. Org. Chem.* 68 (2003) 3433–3438.
- [43] J. McMurry, *Chemistry of Benzene. Organic Chemistry*, Brooks/Cole Publishing Company, Belmont, 1984, pp. 478–515.
- [44] T. Noipa, S. Srijaranai, T. Tuntulani, W. Ngeontae, *Food Res. Int.* 44 (2011) 798–806.